Accepted Manuscript

A Combined Ligand- and Structure-Based approach for the identification of rilmenidine-derived compounds which synergize the antitumor effects of doxorubicin

Jelica Vucicevic, Tatjana Srdic-Rajic, Marco Pieroni, Jonne MM Laurila, Vladimir Perovic, Sabrina Tassini, Elisa Azzali, Gabriele Costantino, Sanja Glisic, Danica Agbaba, Mika Scheinin, Katarina Nikolic, Marco Radi, Nevena Veljkovic

PII: S0968-0896(16)30373-X
DOI: http://dx.doi.org/10.1016/j.bmc.2016.05.043
Reference: BMC 13027

To appear in: *Bioorganic & Medicinal Chemistry*

Received Date: 20 March 2016
Revised Date: 17 May 2016
Accepted Date: 20 May 2016

Please cite this article as: Vucicevic, J., Srdic-Rajic, T., Pieroni, M., Laurila, J.M., Perovic, V., Tassini, S., Azzali, E., Costantino, G., Glisic, S., Agbaba, D., Scheinin, M., Nikolic, K., Radi, M., Veljkovic, N., A Combined Ligand- and Structure-Based approach for the identification of rilmenidine-derived compounds which synergize the antitumor effects of doxorubicin, *Bioorganic & Medicinal Chemistry* (2016), doi: http://dx.doi.org/10.1016/j.bmc.2016.05.043

Graphical Abstract

To create your abstract, type over the instructions in the template box below.
Fonts or abstract dimensions should not be changed or altered.

A Combined Ligand- and Structure-Based approach for the identification of rilmenidine-derived compounds which synergize the antitumor effects of doxorubicin

Leave this area blank for abstract info.

Jelica Vucicevic[a], Tatjana Srdic-Rajic[b], Marco Pieroni[c], Jonne MM Laurila[d], Vladimir Perovic[e], Sabrina Tassini[c], Elisa Azzali[c], Gabriele Costantino[c], Sanja Glisic[e], Danica Agbaba[a], Mika Scheinin[d,f], Katarina Nikolic[a]*, Marco Radi[c]* and Nevena Veljkovic[e]*

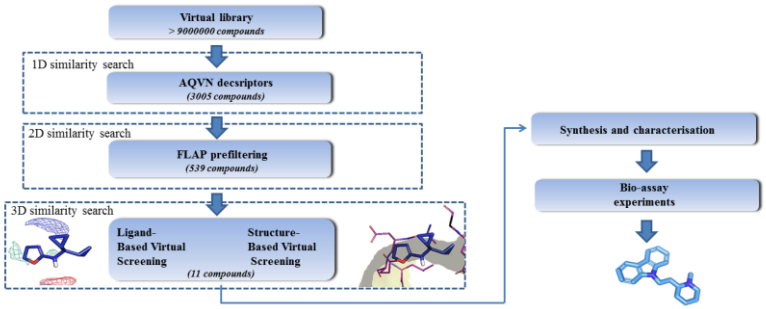

Bioorganic & Medicinal Chemistry
journal homepage: www.elsevier.com

A Combined Ligand- and Structure-Based approach for the identification of rilmenidine-derived compounds which synergize the antitumor effects of doxorubicin

Jelica Vucicevic,[a] Tatjana Srdic-Rajic,[b] Marco Pieroni,[c] Jonne MM Laurila,[d] Vladimir Perovic,[e] Sabrina Tassini,[c] Elisa Azzali,[c] Gabriele Costantino,[c] Sanja Glisic,[e] Danica Agbaba,[a] Mika Scheinin,[d,f] Katarina Nikolic,[a,*] Marco Radi[c,*] and Nevena Veljkovic[e,*]

[a] *Institute of Pharmaceutical Chemistry, Faculty of Pharmacy, University of Belgrade, Vojvode Stepe 450, 11000, Belgrade, Serbia*
[b] *Department of Experimental Oncology, Institute for Oncology and Radiology of Serbia, Pasterova 14, 11000, Belgrade, Serbia*
[c] *P4T Group, Dipartimento di Farmacia, Università degli Studi di Parma, Viale delle Scienze, 27/A, 43124 Parma, Italy*
[d] *Department of Pharmacology, Drug Development and Therapeutics, University of Turku, Kiinamyllynkatu 10, FI-20520 Turku, Finland*
[e] *Center for Multidisciplinary Research, Institute of Nuclear Sciences Vinca, University of Belgrade, Mihaila Petrovica Alasa 14, 11001, Belgrade, Serbia*
[f] *Unit of Clinical Pharmacology, Turku University Hospital, Turku, Finland*

ARTICLE INFO

Article history:
Received
Received in revised form
Accepted
Available online

Keywords:
Drug design
Synthesis
Rilmenidine
Doxorubicin synergism
α_2-Adrenoceptors
Cytotoxic activity
Apoptosis

ABSTRACT

The clonidine-like central antihypertensive agent rilmenidine, which has high affinity for I1-type imidazoline receptors (I1-IR) was recently found to have cytotoxic effects on cultured cancer cell lines. However, due to its pharmacological effects resulting also from α_2-adrenoceptor activation, rilmenidine cannot be considered a suitable anticancer drug candidate. Here, we report the identification of novel rilmenidine-derived compounds with anticancer potential and devoid of α_2-adrenoceptor effects by means of ligand- and structure-based drug design approaches. Starting from a large virtual library, eleven compounds were selected, synthesized and submitted to biological evaluation. The most active compound **5** exhibited a cytotoxic profile similar to that of rilmenidine, but without appreciable affinity to α_2-adrenoceptors. In addition, compound **5** significantly enhanced the apoptotic response to doxorubicin, and may thus represent an important tool for the development of better adjuvant chemotherapeutic strategies for doxorubicin-insensitive cancers.

1. Introduction

Centrally acting hypotensive imidazoline derivatives, such as clonidine, rilmenidine and moxonidine, inhibit the activity of the sympathetic nervous system by activating α_2-adrenoceptors in the brain and possibly also via actions mediated by non-adrenergic I_1-imidazoline receptors (I_1-IR).[1-4] The prototypical agent, clonidine, has almost similar affinity for both types of receptors, whereas the newer antihypertensive agents moxonidine and rilmenidine bind more avidly I_1-IR than α_2-adrenoceptors. Possibly for this reason, they are less prone to elicit the typical side effects of clonidine, i.e. sedation, dry mouth and bradycardia. Recently, imidazoline derivatives have been also found to have other important biological effects not related to cardiovascular regulation, such as control of apoptosis and cell proliferation, both observed in vitro at micro- to millimolar concentrations (Fig. 1). Aceros et al.[5] reported that moxonidine, a moderately efficacious I_1-IR agonist, exerts proapoptotic effects in fibroblasts and anti-apoptotic effects in cardiomyocytes. The imidazoline compound RX871024 induces cell death in insulin-secreting MIN6 cells.[6] S43126, an I_1-IR selective inhibitor of PC12 cell growth, caused considerable dose-dependent cell death, and apoptotic body formation after 72 h of treatment.[7] Our previous study demonstrated that rilmenidine induces significant membrane dissipation and deactivation of the Ras/MAP kinases ERK, p38 and JNK in cultured human leukemic K562 cells, thus exhibiting proapoptotic and antiproliferative effects[8]. However, our incomplete knowledge of I_1-IR signaling pathways and the lack of an I_1-IR crystallographic structure did not allow us to claim unequivocally which is the actual target through which rilmenidine exerts these effects. We have assumed that the action of rilmenidine is connected with its binding to the I_1-IR candidate nischarin and its interaction partner RAC1, a member of the Rac subfamily of Rho guanosine

* Corresponding authors: Nevena Veljkovic, (POB 522, Mihaila Petrovica Alasa 14, 11001, Belgrade, Serbia, E-mail: nevenav@vinca.rs); Marco Radi (Viale delle Scienze, 27/A, 43124 Parma, Italy, E-mail: marco.radi@unipr.it); Katarina Nikolic (Vojvode Stepe 450, 11000, Belgrade, Serbia, E-mail: knikolic@pharmacy.bg.ac.rs.)

triphosphatases (GTPases). Nischarin is a cytoplasmic protein[9] which besides rilmenidine binds numerous other imidazoline ligands and affects cellular signaling cascades controlling cell survival, growth and migration.[10,11] Along with the proapoptotic and antiproliferative effects, we discovered that the I_1-IR agonist rilmenidine rendered leukemic K562 cells, which are particularly resistant to many DNA-damaging chemotherapeutic agents, susceptible to the effects of doxorubicin.[8]

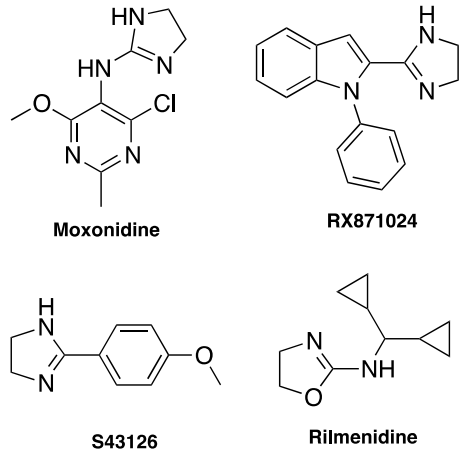

Figure 1. Structures of imidazoline compounds that regulate cellular apoptosis and proliferation in vitro

Doxorubicin, an anthracycline drug, is one of the most effective anticancer drugs ever developed, and although in clinical use for more than 30 years, it still plays an important role in the treatment of many hematological cancers (leukemias and lymphomas) and several types of solid tumors (carcinomas and sarcomas).[12] The therapeutic potential of doxorubicin is significantly limited by the risk of cardiotoxicity, which is dependent on the cumulative dose/treatment schedule and unpredictably evolves towards congestive heart failure. To avoid this serious complication, the maximum recommended cumulative dosage of doxorubicin has been set at 500 mg/m^2.[13] Regardless, doxorubicin cardiotoxicity may occur at lower cumulative doses if co-administered with other antitumor agents (e.g. paclitaxel, trastuzumab). These combined treatment modalities clearly offer improved response rates, but important cardiotoxicity may surface with cumulative doses of doxorubicin as low as 360-400 mg/m^2.[14,15] In the current study, we aimed at extending our earlier investigation on the rilmenidine binding site and I_1-IR candidate nischarin.[16] We used a combined ligand- and structure-based virtual screening approach to identify ligands that, similarly to rilmenidine, could establish effective interactions with nischarin and affect cell viability. In addition, by using nischarin as a target for structure-based virtual screening, we aimed at diminishing ligand binding to α_2-adrenoceptors. Exploring a large in-house virtual library, eleven hit compounds emerged as best candidates. Biological studies confirmed that the most active compound **5** indeed induces apoptosis and sustains the proliferation of K562 cells in a similar fashion as rilmenidine but with limited effects on α_{2A}-adrenoceptors. More importantly, we demonstrated that co-treatment with compound **5** and doxorubicine promotes substantial enhancement of the apoptotic responses of K562 cells compared to the single agents. This integrated medicinal chemistry study provides biologists and pharmacologists with a tool that may represent a promising starting point for the exploration of the I_1-IR pathway and for the development of improved adjuvant chemotherapeutic strategies for cancers with limited susceptibility to doxorubicin.

2. Results and discussion

Here we report the development of a novel virtual screening protocol for the identification of structurally diverse I_1-IR agonists with proapoptotic and antiproliferative activity. To limit the number of hits to be tested, the method included the use of an average quasi-valence number (AQVN)-similarity search, and ligand- and structure-based virtual screening approaches. This combination of techniques allowed us to select eleven different compounds for biological evaluation.

2.1. Chemoinformatic screening

Strong correlations between biological activities of organic molecules and the values of AQVN and electron ion interaction potential (EIIP) chemical descriptors related to long-range interaction properties have been observed.[17] In line with this principle, we proposed a simple criterion to discriminate the biologically relevant chemical space based on AQVN and EIIP. Previously, we demonstrated that 92.5% of about 45 million compounds from the PubChem database are homogeneously distributed within the AQVN interval (2.4 – 3.3). Recently, we reported the selection of HIV and Ebola inhibitors by means of AQVN- and EIIP-similarity searches together with other complementary VS approaches.[18,19] Here, we define an AQVN-based filter for the rapid in silico prescreening of large chemical libraries in order to identify novel rilmenidine analogues. For this purpose, we established the filter by expanding the area centered at rilmenidine's AQVN value (2.4828) to capture 20% of the AQVN space occupied by the I_1-IR agonists reported in the literature (Supplementary material). In this way we defined the rilmenidine AQVN space between 2.4296 and 2.5025. Filtering of compound sets described in the Methods section led to the pre-selection of 3005 compounds that were further investigated in a ligand- and structure-based virtual screening (Fig. 2).

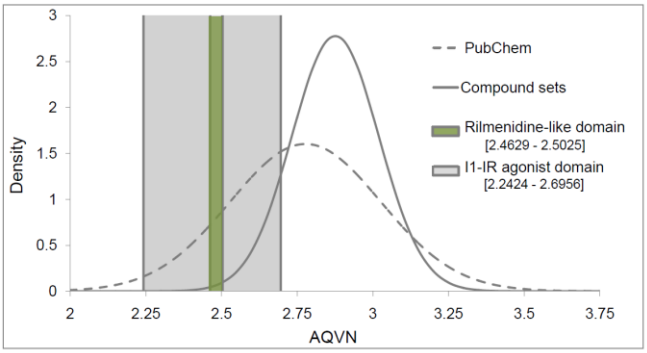

Figure 2. Compound distribution according to their average quasi-valence number (AQVN). 10.47% of the elements from the compound set described in the Methods section are within the I1-IR agonist domain. The compound sets contain 3005 elements within the rilmenidine-like domain.

2.2. Ligand- and Structure-Based Virtual Screening

A number of successful applications of FLAP (fingerprint for ligands and proteins) for the identification of G-protein-coupled receptor ligands have been recently reported.[20-23] However, to our knowledge, this is the first work reporting the application of VS approaches in order to disclose selective I_1-IR ligands with potential proapoptotic and antiproliferative activity. In this work we applied combined ligand- and structure-based virtual screening in order to take into account the variety of available chemical and biological information.[24] After AQVN-based filtering of the in-house virtual library (more than 9×10^6

compounds), the remaining library contained 3005 structurally diverse compounds. We then performed FLAP prefiltering to select only a subset of structures that are enriched in pharmacophore similarity to the template. FLAP fingerprint similarity was used to rank compounds with regard to similarity with rilmenidine. 539 top-ranked substances were selected according to their Glob-Sum values (> 0.01). An enriched dataset constituted by 21 I_1-IR agonists and 539 prefiltered rilmenidine-derived compounds was built and subjected to further ligand- and structure-based virtual screening. The results were estimated in terms of enrichment factors and AUC. As a first step, ligand-based VS was applied to evaluate the similarity between active and untested compounds from the FLAP database and rilmenidine taking into account GRID MIF interaction probes. Various similarity scores corresponding to overlapping MIFs, as well as their combinations, were generated for each molecule. The second screening was performed using a structure-based approach established on the structural homology model of nischarin.[16] The predicted active center of this modelled protein was used to screen the FLAP database considering the similarity between the MIFs of the binding pocket and the ligands. According to the obtained AUC and enrichment factor values, H*DRY*H and H similarity scores were able to efficiently discriminate 21 known active I_1-IR ligands from untested FLAP database compounds in ligand- and structure-based virtual screening studies, respectively, indicated by highest virtual accuracy (AUCLBVS = 1.00; EF1%LBVS = 100 %; AUCSBVS = 0.991; EF1%SBVS = 100 %). Based on the obtained results it can be concluded that shape and hydrophobic interactions are important for activity of compounds toward nischarin. Eleven potential hits (see section 2.3) that had both H scores higher than 0.65 according to the structure-based VS and H*DRY*H scores higher than 0.1 according to the ligand-based VS were selected, synthesized and then tested *in vitro* against K562 cells (Table 1).

2.3. Synthesis of the selected hit compounds

Briefly, for the synthesis of compounds **3a-i**, the commercially available precursor 4-hydroxy-6-methyl-2-pyrone **1** was reacted with the suitable amine at reflux to give the N-substituted pyridinones **2a-d** in good overall yields. Pyridinones **2a-d** were further substituted at C4 with the suitable alkyl- or arylamines under microwave-assisted conditions. Compounds **3a-i** were obtained in acceptable overall yields after purification by flash column chromatography (Scheme 1). Compounds **5** and **7** were prepared according to a protocol already reported elsewhere (Scheme 2).[25]

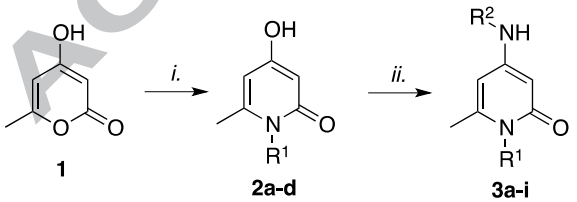

2a: R^1 = isobutyl
2b: R^1 = pentyl
2c: R^1 = isopentyl
2d: R^1 = benzyl

3a: R^1 = isobutyl, R^2 = 4-CF_3benzyl
3b: R^1 = pentyl, R^2 = pentyl
3c: R^1 = pentyl, R^2 = benzyl
3d: R^1 = pentyl, R^2 = 4-Clbenzyl
3e: R^1 = isopentyl, R^2 = isopentyl
3f: R^1 = isopentyl, R^2 = benzyl
3g: R^1 = isopentyl, R^2 = 4-Clbenzyl
3h: R^1 = benzyl, R^2 = pentyl
3i: R^1 = benzyl, R^2 = isopentyl

Scheme 1. Reaction conditions: *i.* R^1-NH_2, H_2O, reflux, 12 h; *ii.* R^2-NH_2, DME, MW, 120 °C, 40 min

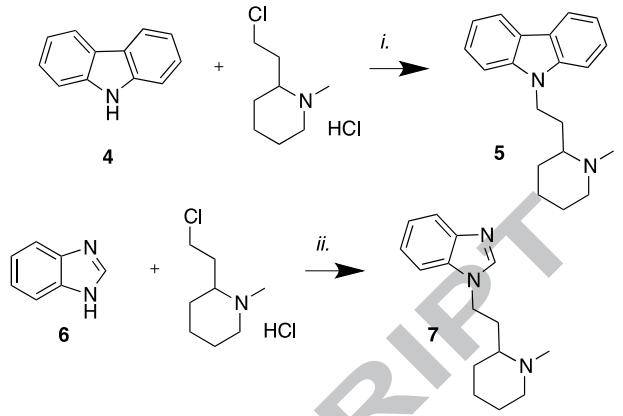

Scheme 2. Reaction conditions: *i.* NaH, DMF, reflux, 48 h

2.4. Characterization of ligands at human α_{2A}-adrenoceptors

The apparent affinities of the eleven hit compounds and those of the reference compounds rilmenidine and efaroxan to human α_{2A}-adrenoceptors were determined using competition binding assays (Table 2). Adrenaline, dexmedetomidine, clonidine and atipamezole, ligands known to bind to α_2-adrenoceptors with high affinity, were used as positive controls in the assays. Among the imidazoline drugs, efaroxan was found to bind α_{2A}-adrenoceptors with relatively high affinity in comparison to clonidine and rilmenidine. None of the eleven rilmenidine-derived hit compounds exhibited appreciable affinity toward human α_{2A}-adrenoceptors, with the possible exception of compounds **5** and **7** (K_i 1.2 and 11 µM). In terms of functional activity, [^{35}S]GTPγS binding experiments were conducted to compare agonist potency and intrinsic activity at recombinant human α_{2A}-adrenoceptors. The results indicated that, similarly to clonidine, rilmenidine is a partial agonist of α_{2A}-adrenoceptors, but with lower potency compared with clonidine. None of the hit compounds nor the α_2-adrenoceptor antagonist efaroxan exhibited agonist-like properties towards the human α_{2A}-adrenoceptor. Some of the rilmenidine-derived compounds produced small negative intrinsic activity values in the functional assay, possibly acting like weak inverse agonists at α_{2A}-adrenoceptors, albeit at very high concentrations.

2.5. Evaluation of Cytotoxicity

K562 cells were exposed to various concentrations of investigated compounds for 48 hours and the cytotoxicity was determined using the MTT assay. It was observed that six compounds exhibited cytotoxic activity at mid- to high micromolar concentrations (Fig. 3). By comparing the effects of compound **5** and the imidazoline compounds (rilmenidine, moxonidine and efaroxan) on cell viability [5,8,26] and apoptosis in K562 cells (Table 3) it was possible to propose compound **5** as a novel hit compound. In the apoptosis assay, rilmenidine induced apoptosis at IC_{50} concentration, as we previously reported, whereas efaroxan and moxonidin were incapable of inducing apoptosis at concentrations as high as 300 µM (Supplementary material).

2.6. Evaluation of the capability of compound 5 to induce apoptosis alone and in combination with doxorubicin

The proapoptotic effect of compound **5** is reflected by the increase of early apoptotic cells in comparison to the vehicle control. We also observed that compound **5** is two-fold more efficient than rilmenidine in inducing cell death (Fig. 4A). FACS was used to evaluate K562 cell cycle

Table 1. Structure and antiproliferative activity (IC_{50}) on K562cells of compounds selected by the VS protocol

Compound	Structure	IC_{50} (μM)
rilmenidine	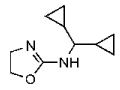	65
efaroxan	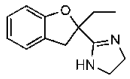	>300
3a	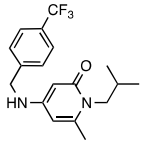	222
3b	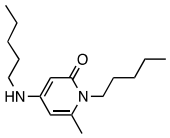	115
3c	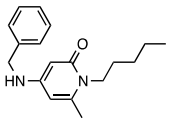	>300
3d	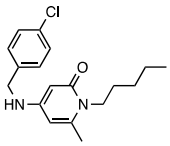	>300
3e	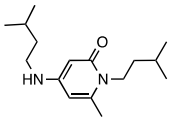	128
3f	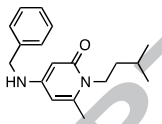	>300
3g	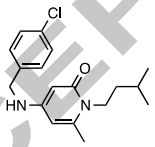	224
3h	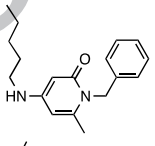	140
3i	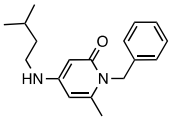	>300
5	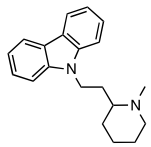	70
7	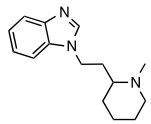	>300

Table 2. Competition binding affinities (K_i) of tested ligands obtained with [^{3}H]RS79948-197 at human α_{2A}-adrenoceptors expressed in CHO cells and estimates of their agonist potency (pEC_{50}) and intrinsic activity obtained with the functional [^{35}S]GTPγS binding assay.

Compound	K_i (nM)[a]	pEC_{50}	Intrinsic activity[b] (% of adrenaline)
3a	58 000 (20 000-170 000)	n.d.	-6 ± 2
3b	62 000 (27 000-150 000)	n.d.	-18 ± 3
3c	41 000 (22 000-80 000)	n.d.	-12 ± 4
3d	80 000 (24 000-270 000)	n.d.	0 ± 4
3e	52 000 (15 000-430 000)	n.d.	-17 ± 4
3f	27 000 (8 100-130 000)	n.d.	-10 ± 2
3g	99 000 (40 000-250 000)	n.d.	-1 ± 4
3h	110 000 (44 000-300 000)	n.d.	-8 ± 5
3i	110 000 (67 000-1100 000)	n.d.	-2 ± 1
5	1 200 (540-3000)	n.d.	-3 ± 2
7	11 000 (3 900-36 000)	n.d.	-6 ± 1
Adrenaline	160 (67-430)	7.52 ± 0.07	100
Rilmenidine	300 (170-520)	6.75 ± 0.07	54 ± 4
Efaroxan	4.4 (2.7-6.9)	n.d.	-13 ± 2
Clonidine	28 (16-48)	7.52 ±	41 ± 6
Dexmedetomidine	2.5 (1.6-3.9)	8.67 ± 0.04	63 ± 3
Atipamezole	1.2 (0.77-2.0)	n.d.	*n.d.*

[a]The apparent K_i (nM) and its 95% confidence intervals are from 3-6 independent experiments, analyzed using a one-site competition mode; [b]Intrinsic activity values are relative to the natural full agonist adrenaline. Values shown for pEC_{50} (negative logarithm of the ligand concentration (nM) causing 50% of the maximal observed agonist effect) and intrinsic activity are means ± s.e.m. from 3-5 independent experiments. n.d. indicates "not determined" for compounds which did not show any agonist activity in the functional assay.

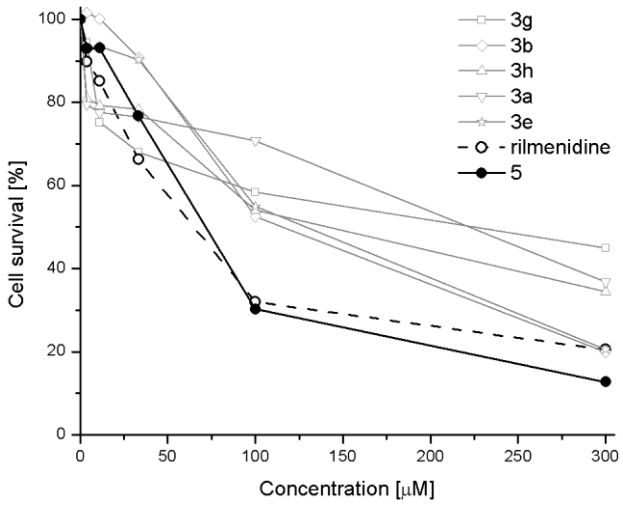

Figure 3. Dose-response cytotoxicity curves of rilmenidine and six novel compounds (**3a**, **3b**, **3e**, **3g**, **3h**, **5**) obtained with the MTT assay in K562 cells after 48 hours.

progression after 48 hours of continual incubation with compound **5**. The accumulation of cells in sub-G1 phase was in concordance with the observed apoptosis (Fig. 4B). To assess the antiproliferative effect of compound **5**, we performed a clonogenic assay of K562 cells in methylcellulose. Compound **5**

inhibited in a dose-dependent manner colony formation of K562 cells after 24h treatment. We observed a significant growth inhibition of 88±6 % at compound **5** IC_{50} concentration (Fig. 4C). Then we counter-screened compound **5** against two non-related oncogenic targets, Abl and Src kinases, in order to asses that these cellular effects were not related to some non-specific activity or compound **5** aggregation. Indeed, no inhibition of selected kinases was observed when compound **5** was tested both in the presence and absence of detergent in the reaction mixture (Supplementary material). Furthermore, in silico analysis by the Aggregator Advisor server[27] did not find any similarity between compound **5** and any known aggregator listed in their database. These results tend to exclude aggregation effects or non-specific activities of compound **5**, suggesting that the dose-dependent cytotoxic effect observed is strictly linked to the specific action on the I1-IR pathway.

K562 is a model cell line of blast-like chronic myeloid leukemia which is relatively insensitive to apoptosis induced by DNA damaging drugs, including doxorubicin.[28] We have previously demonstrated that combined application of rilmenidine and doxorubicin synergistically sensitized K562 cells to apoptosis in comparison with doxorubicin alone (44% vs. 10%).[8] Here, we examined the combined application of compound **5** and doxorubicin and observed enhanced cytotoxicity and apoptotic responses of K562 cells compared to doxorubicin alone (Fig. 5). The IC_{50} of doxorubicin in K562 cells was 1.0 μM. To assess the cytotoxic effects of the drug combination, we used a fixed molar ratio of compound **5**/doxorubicin of 70:1, as required by the Chou-Talalay method (Table 4). CI values significantly <1 observed over the range of tested concentrations indicated strong synergistic effects. Similar, albeit weaker, synergism has been previously demonstrated with rilmenidine.[8] Compound **5** is a carbazole derivative. Many natural and semi-synthetic carbazoles show promising antitumor activity against different cancer cell lines[30-32], often by inhibiting DNA-dependent enzymes and by causing DNA damage. Recently, it was shown that the carbazole derivative MHY407 sensitizes breast cancer cells to doxorubicin and etoposide toxicity by increasing DNA damage-related proteins and inducing S phase arrest.[33] Here, cell cycle experiments showed

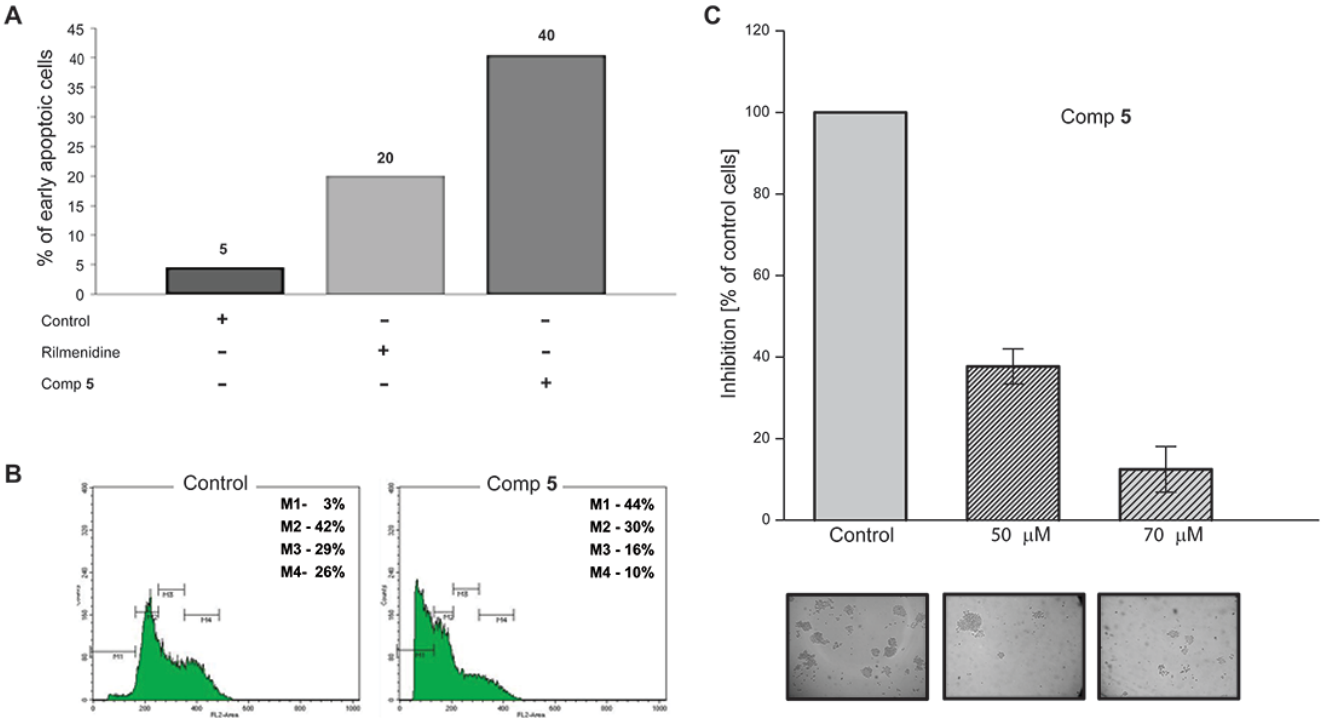

Figure 4. Induction of apoptotic cell death and proliferation inhibition in K562 cells treated with compound 5. (A) Early apoptosis in K562 cells treated with vehicle, 50μM rilmenidine and 70 μM compound **5** after 48 hours. (B) Effect of compounds on cell cycle phase distribution. Cells were treated with 70 μM compound **5** for 48 hours. After the indicated time, the cells were stained with PI and analyzed for alternations in cell cycle phase distribution by flow cytometry. The results are representative of three independent experiments. M1 - Cells with DNA content corresponding to sub-G1 peak; M2- Cells with DNA content corresponding to G0/G1 phases. M3 - Cells with DNA content corresponding to the S phase. M4 - Cells with DNA content corresponding to G2/M phases. (C) Compound **5** dose-dependently inhibited K562 colony formation after 24 hour treatment (upper panel). Images of representative plates of the K562 cell line incubated with 50 μM and 70 μM compound **5** (lower panel).

Table 3. Concentrations of imidazoline and imidazoline-like compounds that induce cell death in the K562 cell line

Compound	Antiproliferative/proapoptotic concentration (μM)
Rilmenidine	50
Moxonidine	>300
Efaroxan	-
Compound 5	**70**

Table 4. Combination index (CI) value of the combination treatment with compound **5** and doxorubicin at a molar ratio of 70:1[29]

Compound 5 (μM)	doxorubicin (μM)	Inhibition rate (%)	CI
25	0.36	45.75	0.877
50	0.7	68.62	0.511
70	1.0	72.21	0.617
100	1.4	78.21	0.688

that the synergistic effect obtained by combining the carbazole derivative **5** and doxorubicin is connected to the recovery of doxorubicin induced G2/M arrest. As depicted in Fig. 6, cells treated with doxorubicin accumulate in G2/M phase, whereas co-treatment significantly decreased G2/M phase accumulation on account of an increased sub-G1 cell population.

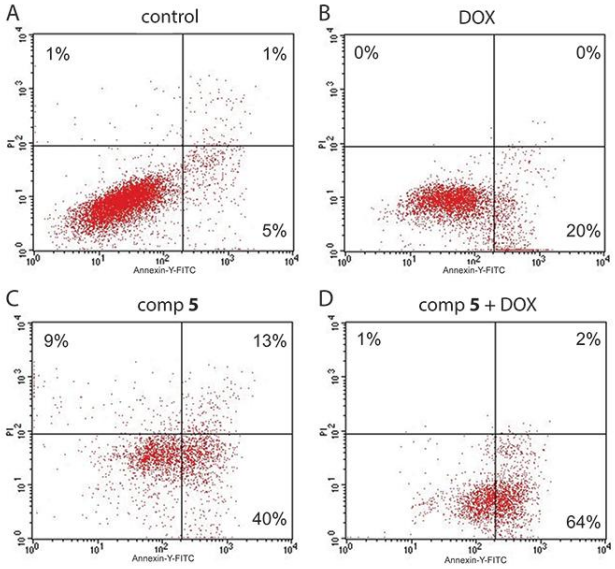

Figure 5. Induction of apoptotic cell death in K562 cells. Proportion of early apoptotic (FITC+/PI-) cells in a population was measured by bivariate Annexin V/PI flow cytometry in untreated K562 cells (A) and in cells treated with 70 μM compound 5 (B), 1 μM doxorubicin (C), and compound 5 plus doxorubicin (D) after 48 hours.

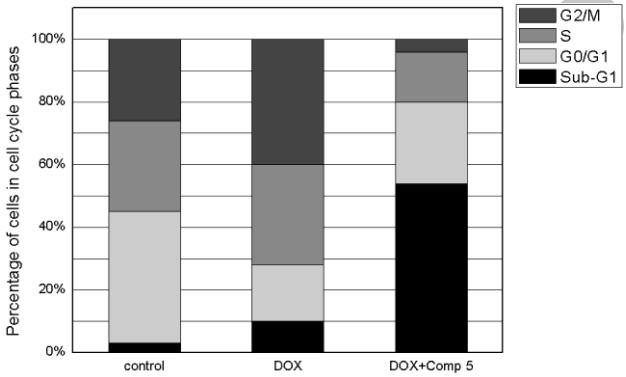

Figure 6. Effect of DOX and DOX/**5** combination on cell cycle phase distribution of K562 cells. The numbers indicate the fraction of cells in a given phase of the cell cycle.

3. Conclusions

In this work, which extends our previous investigation on the nischarin-rilmenidine binding site, we aimed at understanding the structure activity relationship underlying the observed proapoptotic activity of rilmenidine. We sought to identify novel compounds with rilmenidine-like activity and mechanism of action but with different chemical structure. We used a VS protocol that includes AQVN calculations accounting for the long-range properties of organic molecules and combined ligand- and structure-based virtual screening protocols based on GRID MIF similarities between tested compounds and the template rilmenidine. Among eleven prospective candidates that stemmed from the in silico screening experiments, compound **5** was found to be the most active derivative with cytotoxic activity against K562 cells comparable to that of rilmenidine. In addition, none of the identified eleven compounds showed any detectable agonist activity at recombinant human α_{2A}-adrenoceptors, suggesting that unwanted side effects mediated by the activation of this receptor may be avoided. Consistently with the observed apoptosis, the flow cytometric analysis of cell cycle progression showed an increase in the proportion of K562 cells in the sub-G1 phase, complemented with decreased proportions of cells in G1, S and G2/M. Previously, we have also shown that rilmenidine rendered K562 cells, which are particularly resistant to chemotherapeutic agents, susceptible to the DNA damaging drug doxorubicin. Similarly, combined treatment with compound **5** and doxorubicin showed synergistic increases in apoptosis compared to doxorubicin alone (64% vs. 20%), which highlighted the potential of compound **5** or its derivatives to complement conventional chemotherapeutic regimens through improved antitumor efficacy and possibly reduced side effects. In conclusion, the integrated medicinal chemistry study herein reported provides biologists and pharmacologists with a novel tool (compound **5**) that may represent a promising starting point for the exploration of the I1-IR pathway and for the development of better adjuvant chemotherapeutic strategies for cancers with limited susceptibility to doxorubicin-like agents.

Experimental

4.1. Compound sets

The virtual library used for *in silico* screening was composed of the P4T-group's internal collection plus a focused virtual library generated on the basis of a versatile multicomponent synthetic protocol.[34] This synthetic sequence was used as input for the Smi-Lab software[35] to combine a series of commercial building blocks. The complete virtual library contained more than 9×10^6 compounds.

4.2. Virtual screening protocol

The virtual screening (VS) protocol used in this study was based on the combination of different methods. In the beginning of the multi-step screening process we used average quasi-valence number (AQVN) similarity searches to reduce the number of hits. Further parallel ligand- and structure-based screening protocols were run independently and the hits that showed good ranking in both approaches were selected for biological testing.

4.2.1. Chemoinformatics screen

Molecular descriptor AQVN was calculated as described in [17] using the FormCal computational tool.[36] Values of AQVN of rilmenidine and 28 I_1-IR agonists (Supplementary material) selected from the literature were used to define filtering domains for hit-like compounds.

4.2.2. Ligand and Structure Based Virtual Screening Protocols

The software FLAP (Fingerprints for Ligand and Proteins) 1.0.0 [20,37] was used to perform both ligand- and structure-based virtual screening in order to find novel I_1-IR ligands with antiproliferative/proapoptotic activity. The parallel application of these two VS methods was expected to produce structurally diverse hits with the desired biological activity.

4.2.2.1. FLAP database generation

During the FLAP database creation, the 3D structures of compounds from the virtual library were generated using molecular mechanistic MM3 force fields. The database was enriched with rilmenidine and 20 I_1-IR agonists with a reported p*K*i > 6 as an affinity cutoff (Supplementary material). For each ligand, up to 25 conformers were generated with root-mean-

square deviation (RMSD) lower than 0.3 Å. GRID molecular interaction fields (MIFs) were calculated for each conformer and translated into the fingerprints on which all FLAP screening calculations were based. The GRID probes H, DRY, O, and N1 are used to describe shape, hydrophobic interaction, H-bond acceptors and H-bond donor interactions of molecules, respectively. Charge is implicitly described by the magnitude of the interaction using the N1 and O probes.

4.2.2.2. FLAP Virtual Screening Analysis

In LBVS, compounds from the virtual library were ranked according to their similarity with rilmenidine (*ChEMBL289480*), while in SBVS they were ranked according to the active site of nischarin, taking into account GRID MIFs. Probe scores (representing the degree of overlap of the MIFs for each probe individually as well as for their combinations), distance scores (representing overall difference of probe scores between the ligand and the template) and two global scores (Glob-Prod and Glob-Sum) were applied to quantify similarity. All similarities ranged from 0.0 (bad) to 1.0 (good), except for the distance score, where 0.0 represented good.[38] Since an X-ray crystallography structure of nischarin was not available, a recently published homology model was used in this study.[16] Automatic identification of binding pockets of proteins was performed using the *FLAPsite* pocket detection algorithm.[21]

4.2.2.3. Virtual Screening Evaluation

The results of the VS protocol were examined in terms of enrichment factor (EF) and the area under curve (AUC) of the receiver operator characteristic (ROC) curve. A ROC curve is a plot of the true positive rate (y-axis) against the false positive rate (x-axis) for a ranked series of molecules. AUC of 0.5 corresponds to random discrimination between actives and untested compounds (decoys), whereas an AUC of 1.0 corresponds to an ideal case, in which all known true actives are ranked before untested compounds (decoys). EF is a cumulative plot of the percentage of true positives (y-axis) vs. percentage of the whole dataset (x-axis) for a ranked series of molecules. The $EF_{X\%}$ indicates the EF values retaining the X% of the whole database.[39]

3.3. Chemistry

All reagents were purchased from Sigma-Aldrich, Alfa-Aesar and Enamine at reagent purity and, unless otherwise noted, were used without any further purification. Dry solvents used in the reactions were obtained by distillation of technical grade materials over appropriate dehydrating agents. MCRs were performed using CEM Microwave Synthesizer-Discover model. Reactions were monitored by thin layer chromatography on silica gel-coated aluminium foils (silica gel on Al foils, SUPELCO Analytical, Sigma-Aldrich) at both 254 and 365 nm wavelengths. Where indicated, intermediates and final products were purified through silica gel flash chromatography (silica gel, 0.040-0.063 mm), using appropriate solvent mixtures. ^{1}H-NMR were recorded on a BRUKER AVANCE spectrometer at 400 and 300 MHz, whereas ^{13}C-NMR spectra were recorded in the same instrument at 100.6 MHz. TMS was used as the internal standard. ^{1}H-NMR spectra are reported in this order: multiplicity and number of protons. Standard abbreviations indicating the multiplicity were used as follows: s = singlet, d = doublet, dd = doublet of doublets, t = triplet, q = quadruplet, m = multiplet and br = broad signal. HPLC/MS experiments were performed with an Agilent 1100 series HPLC system, equipped with a Waters Symmetry C18, 3.5 µm, 4.6 mm x 75 mm column and an Applied Biosystem/MDS SCIEX MS detector equipped with an API 150EX ion source. HRMS experiments were performed with LTQ ORBITRAP XL THERMO.

3.3.1. General procedure for the synthesis of compounds 2a-d:

A mixture of 4-hydroxy-6-methyl-2-pyrone **1** (500 mg, 3.96 mmol) and isobutylamine (394.0 µL, 3.96 mmol, for **2a**) or pentylamine (459.6 µL, 3.96 mmol, for **2b**) or isopentylamine (459.6 µL, 3.96 mmol, for **2c**) or benzylamine (432.6 µL, 3.96 mmol, for **2d**) in water (16 mL) was stirred under reflux for 12 hours. At the end of the reaction the mixture was cooled to room temperature. The solid mass was filtrated under vacuum, washed with diethyl ether and purified by silica gel flash chromatography (dichloromethane/methanol from 99/1 to 95/5) to give the desired compounds as white solids.

4-hydroxy-1-isobutyl-6-methylpyridin-2(1*H*)-one (2a). (90% yield). ^{1}H NMR (300 MHz, DMSO-d_6) δ 10.30 (s, 1H), 6.05 (s, 1H), 5.95 (s, 1H), 3.83-3.82 (m, 2H), 2.34 (s, 3H), 2.21-2.14 (m, 1H), 0.94 (d, *J* = 6.5 Hz, 6H). MS (ESI) *m/z* 182.2 $[M + H]^+$, 204.3 $[M + Na]^+$.

4-hydroxy-6-methyl-1-pentylpyridin-2(1*H*)-one (2b). (79%yield). ^{1}H NMR (300 MHz, DMSO-d_6) δ 10.32 (s, 1H), 5.98 (s, 1H), 5.91 (s, 1H), 3.96-3.91 (m, 2H), 2.34 (s, 3H), 1.67-1.62 (m, 2H), 1.37-1.32 (m, 4H), 0.93-0.89 (m, 3H). MS (ESI) *m/z* 196.4 $[M + H]^+$, 218.4 $[M + Na]^+$.

4-hydroxy-1-isopentyl-6-methylpyridin-2(1*H*)-one (2c). (83% yield). ^{1}H NMR (300 MHz, DMSO-d_6) δ 10.32 (s, 1H), 5.73 (s, 1H), 5.47 (s, 1H), 3.86-3.80 (m, 2H), 2.29 (s, 3H), 1.65-1.56 (m, 1H), 1.41-1.34 (m, 2H), 0.91 (d, *J* = 6.6 Hz, 6H). MS (ESI) *m/z* 196.2 $[M + H]^+$, 218.3 $[M + Na]^+$.

1-benzyl-4-hydroxy-6-methylpyridin-2(1*H*)-one (2d). (89% yield). ^{1}H NMR (300 MHz, DMSO-d_6) δ 10.31 (s, 1H), 7.36-7.26 (m, 5H), 5.54 (s, 1H), 5.47 (s, 1H), 4.25 (d, *J*= 5.3 Hz, 2H), 2.27 (s, 3H). MS (ESI) *m/z* 216.2 $[M + H]^+$, 238.3 $[M + Na]^+$.

3.3.2. General procedure for the synthesis of compounds 3a-i:

In a 10 mL microwave tube, equipped with magnetic stir bar and septum, a mixture of intermediate **2a-d** (0.51 mmol) and the opportune amine (0.77 mmol) in dimethoxyethane (1 mL) was heated at 120 °C for 40 minutes in the microwave apparatus (maximum power input: 300 W; maximum pressure: 250 PSI; power max: OFF; stirring: ON). After cooling to room temperature the solvent was evaporated under reduced pressure and the residue was purified by silica gel flash chromatography (dichloromethane/methanol from 99/1 to 98/2), affording the desired compounds as white solids.

1-isobutyl-6-methyl-4-((4-(trifluoromethyl)benzyl)amino)pyridin-2(1*H*)-one (3a). (29% yield). ^{1}H NMR (400 MHz, $CDCl_3$) δ 7.60 (d, *J* = 7.8 Hz, 2H), 7.42 (d, *J* = 7.8 Hz, 2H), 5.53 (s, 1H), 5.46 (s, 1H), 4.59 (s, 1H), 4.36 (d, *J*= 5.2 Hz, 2H), 3.76-3.74 (m, 2H), 2.27 (s, 3H), 2.20-2.13 (m, 1H), 0.94 (d, *J* = 6.6 Hz, 6H). ^{13}C NMR (100.6 MHz, $CDCl_3$) δ 164.9, 154.2, 145.6, 142.3, 128.0, 127.5 (2C), 125.7 (2C), 125.6, 99.3, 91.8, 50.2, 46.4, 28.1, 20.9, 20.1 (2C). MS (ESI) *m/z* 339.2 $[M + H]^+$, 361.3 $[M + Na]^+$. HRMS (ESI) calculated for C18H21F3N2O [M + H]+ 339.1606, found 339.17022.

6-methyl-1-pentyl-4-(pentylamino)pyridin-2(1*H*)-one (3b). (35%yield). ^{1}H NMR (300 MHz, $CDCl_3$) δ 5.46 (s, 1H), 5.40 (s, 1H), 4.33-4.32 (m, 1H), 3.88-3.82 (m, 2H), 3.05-2.98 (m, 2H), 2.23 (s, 3H), 1.64-1.51 (m, 4H), 1.34-1.28 (m, 8H), 0.90-0.86 (m, 6H). ^{13}C NMR (75 MHz, $CDCl_3$) δ 164.7, 154.8, 144.5, 99.5,

90.4, 43.4, 42.6, 29.3, 29.1, 28.9, 28.6, 22.4, 22.3, 20.3, 14.0, 13.9. MS (ESI) *m/z* 265.4 $[M + H]^+$, 287.3 $[M + Na]^+$. HRMS (ESI) calculated for C16H28N2O [M + H]+ 265.2202, found 265.22899.

4-(benzylamino)-6-methyl-1-pentylpyridin-2(1*H*)-one (3c). (31% yield). ^{1}H NMR (400 MHz, $CDCl_3$) δ 7.36-7.26 (m, 5H), 5.52 (s, 1H), 5.51 (s, 1H), 4.53 (s, 1H), 4.25 (d, *J*= 5.4 Hz, 2H), 3.90-3.86 (m, 2H), 2.27 (s, 3H), 1.65-1.63 (m, 2H), 1.36-1.34 (m, 4H), 0.93-0.90 (m, 3H). ^{13}C NMR (100.6 MHz, $CDCl_3$) δ 164.6, 154.5, 144.9, 137.9, 128.8 (2C), 127.6, 127.5 (2C), 99.3, 91.4, 47.0, 43.6, 29.2, 28.8, 22.5, 20.4, 14.0. MS (ESI) *m/z* 285.2 $[M + H]^+$, 307.2 $[M + Na]^+$. HRMS (ESI) calculated for C18H24N2O [M + H]+ 285.1889, found 285.19052.

4-((4-chlorobenzyl)amino)-6-methyl-1-pentylpyridin-2(1*H*)-one (3d). (32% yield). ^{1}H NMR (400 MHz, $CDCl_3$) δ 7.30 (d, *J* = 7.8 Hz, 2H), 7.23 (d, *J* = 7.8 Hz, 2H), 5.51 (s, 1H), 5.43 (s, 1H), 4.57 (s, 1H), 4.21 (d, *J*= 4.4 Hz, 2H), 3.88-3.84 (m, 2H), 2.27 (s, 3H), 1.65-1.62 (m, 2H), 1.36-1.34 (m, 4H), 0.92-0.89 (m, 3H). ^{13}C NMR (100.6 MHz, $CDCl_3$) δ 164.5, 154.3, 145.0, 136.4, 133.3, 128.9 (2C), 128.7 (2C), 99.3, 91.5, 46.2, 43.6, 29.1, 28.8, 22.5, 20.4, 14.0. MS (ESI) *m/z* 319.3 $[M + H]^+$, 341.4 $[M + Na]^+$. HRMS (ESI) calculated for C18H23ClN2O [M + H]+ 319.1499, found 319.15063.

1-isopentyl-4-(isopentylamino)-6-methylpyridin-2(1*H*)-one (3e). (33% yield). ^{1}H NMR (400 MHz, $CDCl_3$) δ 5.45 (s, 1H), 5.44 (s, 1H), 3.98 (s, 1H), 3.94-3.90 (m, 2H), 3.09-3.05 (m, 2H), 2.27 (s, 3H), 1.74-1.64 (m, 2H), 1.55-1.45 (m, 4H), 0.97 (d, *J* = 6.6 Hz, 6H), 0.94 (d, *J* = 6.6 Hz, 6H). ^{13}C NMR (100.6 MHz, $CDCl_3$) δ 164.6, 154.6, 144.6, 99.4, 90.7, 42.1, 40.9, 37.9, 37.8, 26.5, 25.9, 22.5 (2C), 22.4 (2C), 20.2. MS (ESI) *m/z* 265.3 $[M + H]^+$, 287.2 $[M + Na]^+$. HRMS (ESI) calculated for C16H28N2O [M + H]+ 265.2202, found 265.22951.

4-(benzylamino)-1-isopentyl-6-methylpyridin-2(1*H*)-one (3f). (28% yield). ^{1}H NMR (400 MHz, $CDCl_3$) δ 7.35-7.26 (m, 5H), 5.52 (s, 1H), 5.49 (s, 1H), 4.61 (s, 1H), 4.24 (d, *J*= 5.4 Hz, 2H), 3.92-3.88 (m, 2H), 2.26 (s, 3H), 1.73-1.64 (m, 1H), 1.54-1.48 (m, 2H), 0.97 (d, *J* = 6.6 Hz, 6H). ^{13}C NMR (100.6 MHz, $CDCl_3$) δ 164.5, 154.6, 144.8, 137.9, 128.7 (2C), 128.5, 127.5 (2C), 99.4, 91.3, 46.9, 42.1, 37.8, 26.5, 22.5 (2C), 20.3. MS (ESI) *m/z* 285.3 $[M + H]^+$, 307.3 $[M + Na]^+$. HRMS (ESI) calculated for C18H24N2O [M + H]+ 285.1889, found 285.19034.

4-((4-chlorobenzyl)amino)-1-isopentyl-6-methylpyridin-2(1*H*)-one (3g). (33% yield). ^{1}H NMR (400 MHz, $CDCl_3$) δ 7.32-7.22 (m, 4H), 5.52 (s, 1H), 5.48 (s, 1H), 4.55 (s, 1H), 4.24 (d, *J*= 5.4 Hz, 2H), 3.93-3.89 (m, 2H), 2.28 (s, 3H), 1.73-1.67 (m, 1H), 1.55-1.49 (m, 2H), 0.97 (d, *J* = 6.6 Hz, 6H). ^{13}C NMR (100.6 MHz, $CDCl_3$) δ 164.4, 154.3, 144.9, 136.4, 133.3, 128.9 (2C), 128.7 (2C), 99.3, 91.5, 46.2, 42.2, 37.8, 26.5, 22.5 (2C), 20.3. MS (ESI) *m/z* 319.3 $[M + H]^+$, 341.3 $[M + Na]^+$. HRMS (ESI) calculated for C18H23ClN2O [M + H]+ 319.1499, found 319.15082.

1-benzyl-6-methyl-4-(pentylamino)pyridin-2(1*H*)-one (3h). (31% yield). ^{1}H NMR (400 MHz, $CDCl_3$) δ 7.27-7.14 (m, 5H), 5.54 (s, 1H), 5.49 (s, 1H), 5.25 (d, *J*= 5.4 Hz, 2H), 4.30 (s, 1H), 3.10-3.05 (m, 2H), 2.12 (s, 3H), 1.61-1.59 (m, 2H), 1.34-1.27 (m, 4H), 0.93-0.89 (m, 3H). ^{13}C NMR (100.6 MHz, $CDCl_3$) δ 165.0, 155.0, 145.3, 137.7, 128.6 (2C), 126.9, 126.3 (2C), 99.8, 90.0, 46.0, 42.7, 29.2, 28.6, 22.4, 20.5, 14.0. MS (ESI) *m/z* 285.3 $[M + H]^+$, 307.2 $[M + Na]^+$. HRMS (ESI) calculated for C18H24N2O [M + H]+ 285.1889, found 285.19074.

1-benzyl-4-(isopentylamino)-6-methylpyridin-2(1*H*)-one (3i). (36% yield). ^{1}H NMR (400 MHz, $CDCl_3$) δ 7.30-7.13 (m, 5H), 5.54 (s, 1H), 5.51 (s, 1H), 5.24 (d, *J*= 5.4 Hz, 2H), 4.30 (s, 1H), 3.19-3.07 (m, 2H), 2.12 (s, 3H), 1.67-1.66 (m, 1H), 1.52-1.46 (m, 2H), 0.94 (d, *J* = 6.4 Hz, 6H). ^{13}C NMR (100.6 MHz, $CDCl_3$) δ 165.0, 154.9, 145.4, 137.7, 128.6 (2C), 126.9, 126.3 (2C), 99.8, 90.0, 46.0, 40.9, 37.8, 25.9, 22.5 (2C), 20.5. MS (ESI) *m/z* 285.3 $[M + H]^+$, 307.3 $[M + Na]^+$. HRMS (ESI) calculated for C18H24N2O [M + H]+ 285.1889, found 285.19088.

3.3.3. General procedure for the synthesis of compounds 5 and 7.

Carbazole **4** or benzimidazole **6** (3 mmol) was added at 0 °C to a suspension of sodium hydride (60% dispersion in mineral oil; 8.97 mmol) in dry DMF (15 mL). Reaction mixture was stirred for 15 minutes at the same temperature and then 2-(2-chloroethyl)-piperidine hydrochloride (3.88 mmol) was added portion wise. The mixture was allowed to react at room temperature for 48 hours until consumption of the starting material. After quenching with water (20 ml), the mixture was extracted with ethyl acetate (3 × 10 mL), and the organic layers were washed with water and brine (3 × 10 mL), dried over anhydrous Na_2SO_4 and concentrated under reduced pressure.

9-(2-(1-methylpiperidin-2-yl)ethyl)-9H-carbazole (5). The crude material was purified through silica gel flash chromatography eluting with dichloromethane/methanol 9/1. (Yield: 53%). White powder. ^{1}H NMR ($CDCl_3$-400 MHz) δ 1.36-1.40 (m, 1H), 1.65-1.68 (m, 3H), 1.82-1.85 (m, 2H), 2.07-2.3 (m, 4H), 2.37 (s, 3H), 2.92-2.97 (m, 1H), 4.36-4.48 (m, 2H), 7.24,7.52 (m, 6H), 8.12 (d, J = 8 Hz, 2H). ^{13}C NMR ($CDCl_3$-100.6 MHz) δ 24.2, 25.3, 30.5, 31.4, 35.5, 39.2, 42.7, 56.9, 61.7, 108.5, 118.8, 120.4, 123.0, 125.7, 140.2. MS (ESI) *m/z* 293.3 $[M + H]^+$, 315.4 $[M + Na]^+$. HRMS (ESI) calculated for C20H24N2 [M + H]+ 293.1939, found 293.20123.

1-(2-(1-methylpiperidin-2-yl)ethyl)-1H-benzo[d]imidazole (7). The crude material was purified by flash column chromatography petroleum ether/ethyl acetate 9/1. (Yield: 72%) Yellow oil. 1H-NMR ($CDCl_3$-300 MHz) δ 1.27-1.77 (m, 6H), 2.02-2.20 (m, 4H), 2.30 (s, 3H), 2.86-2.94 (m, 1H), 4.15- 4.36 (m, 2H), 7.20-7.34 (m, 2H), 7.39-7.44 (m, 1H), 7.80- 7.85 (m, 1H), 7.93 (s, 1H). 13C-NMR ($CDCl_3$-100.6 MHz) δ 24.2, 25.1, 30.2, 32.9, 41.3, 42.5, 56.7, 61.1, 64.4, 88.8, 109.6, 120.4, 122.1, 122.9, 142.8. MS (ESI) *m/z* 244.2 $[M + H]^+$, 266.3 $[M + Na]^+$. HRMS (ESI) calculated for C15H21N3 [M + H]+ 244.1735, found 244.18082.

3.4. α_2-Adrenoceptor assays

3.4.1. Cell culture

Recombinant Chinese hamster ovary (CHO) cells (K1 strain) (American Type Culture Collection (ATCC), Manassas, VA, USA), stably expressing the cDNA encoding the human α_{2A}-adrenoceptor subtype, were produced as previously described by Pohjanoksa et al.[40] Cells were cultured in α-minimum essential medium (GIBCO™, Invitrogen, Carlsbad, CA, USA) supplemented with 26 mM $NaHCO_3$, 5% heat-inactivated fetal bovine serum (FBS), penicillin (50 IU/ml), streptomycin (50 µg/ml) and 200 µg/ml G418. The cultured cells were tested for their capacity to bind the α_2-adrenoceptor antagonist radioligand [^{3}H]RS-79948-197 (GE Healthcare, London, U.K.). Confluent cells were harvested into chilled phosphate-buffered saline, pelleted and frozen at –70 °C.

3.4.2. Membrane preparation

All procedures were performed on ice. CHO cell pellets were thawed and suspended in hypotonic lysis buffer (10 mM Tris–

HCl, 0.1 mM EDTA, 0.32 mM sucrose, pH 7.4) and homogenised using an Ultra-Turrax homogeniser (3 × 10 s at 8000 rpm). The homogenate was centrifuged at 180 g for 15 min to remove cell nuclei, unbroken cells and aggregates. The supernatants were pooled and centrifuged at 50,200 g for 30 min. The pellet was washed with TE buffer (10 mM Tris, 0.1 mM EDTA) and re-centrifuged as above. The membranes were then suspended in TE buffer, aliquoted and stored at –70 °C until used. Protein concentrations were determined with the method of Bradford[41] using bovine serum albumin as reference.

3.4.3. [^{35}S]GTPγS binding assay

Agonist-induced stimulation of [^{35}S]GTPγS binding was measured essentially as described previously.[42] Briefly, membranes were thawed and diluted with binding buffer (25 mM Tris, 1 mM EDTA, 5 mM $MgCl_2$, 20 mM NaCl, 1 µM GDP, 1 mM DTT, 30 µM ascorbic acid, pH 7.4). Incubations were performed on 96-well Millipore MultiScreen MSFBN glass-fibre filter plates. Samples containing 5 µg of membrane protein were incubated with 7 or 8 serial dilutions of the test compounds and 0.1 nM [^{35}S]GTPγS (PerkinElmer, Boston, MA, USA). Reactions were terminated after 30 min incubation at RT by rapid vacuum filtration using a Millipore MultiScreen Vacuum Manifold. The filter plates were washed three times with ice-cold wash buffer (20 mM Tris, 1 mM EDTA, 5 mM $MgCl_2$, pH 7.4). Filters were dried and 50 µl SuperMix scintillation cocktail was added into each well. The incorporated radioactivity was measured using a Wallac 1450 Betaplate scintillation counter. All experiments were performed in duplicate and repeated at least three times. Analysis of the results with GraphPad Prism software yielded estimates of agonist potency (EC_{50}) and efficacy (intrinsic activity in comparison to the natural full agonist adrenaline).

3.4.4. Competition binding assays

Competition binding assays were implemented using a MultiScreen Vacuum Manifold system (Millipore) with Millipore MultiScreen MSFBN 96-well glass fibre filtration plates. The experiments were performed in a total assay volume of 180 µl (in 50 mM potassium phosphate buffer, pH 7.4) using 0.2 nM [^{3}H]RS-79948-197 ((8a*R*,12a*S*,13a*S*)-5,8,8a,9,10,11,12,12a,13,13a-dechydro-3-methoxy-12-(ethylsulfonyl)-6*H*-isoquino[2,1-*g*][1,6]naphthyridine; GE Healthcare, London, U.K.), 8 serial dilutions of the competitor ligands and crude cell membrane preparations containing 10 µg of protein per sample. Non-specific binding was determined in parallel wells in the presence of 100 µM oxymetazoline. Bound radioactivity was measured with a Wallac 1450 MicroBeta scintillation counter (PerkinElmer Wallac). All experiments were performed in duplicate and repeated at least three times. The apparent affinity (apparent K_i) of each ligand was determined using nonlinear regression analysis (GraphPad Prism), assuming one-site binding. For conversion of IC_{50} estimates to K_i values, the Cheng-Prusoff equation was applied.[43]

3.5. Evaluation of antiproliferative and proapoptotic activity

3.5.1. Cell culture

Human chronic myelogenous leukemia K562 cells were obtained from ATCC. Cells were maintained in RPMI-1640 medium (Gibco, Grand Island, NY, USA) with 10% heat-inactivated fetal calf serum (FCS, Gibco) at 37°C in 5% CO_2. Nutrient medium RPMI 1640 was prepared in sterile deionized water, supplemented with penicillin (192 IU/mL), streptomycin (200 µg/mL), 4-(2-hydroxyethyl) piperazine-1-ethanesulfonic acid (HEPES) (25 mM), L-glutamine (3 mM) and 10% of heat-inactivated FCS (pH 7.2).

3.5.2. Cytotoxicity assay and combination index (CI)

The cytotoxicity of compounds on K562 cells were measured using the MTT (3-(4,5-dimethylthiazol-2-yl)-2,5-diphenyltetrazolium bromide) assay developed by Mosmann[44] and modified by Ohno and Abe.[45] After treatment in 96-well plates, 20 µL MTT solution was added to each well. Samples were incubated for a further 4 h, followed by the addition of 100 µl of 10% SDS. Absorbance at 570 nm was measured on the following day. To quantify cell survival (S%), the absorbance of a sample with cells grown in the presence of different concentrations of the investigated agents was divided by the absorbance of the control cells grown only in the nutrient medium, and multiplied by 100. The absorbance of the blank was subtracted from the corresponding absorbance of samples with target cells. The IC_{50} value is the concentration of the agent that inhibited cell survival by 50%, compared to the vehicle-treated control. IC_{50} was calculated as described in [46]. As a positive control we used rilmenidine hemifumarate salt (prod. no. R134) and as a negative control, efaroxan hydrochloride (prod. no. E3263) (Sigma-Aldrich). To assess the cytotoxic effects of drug combinations, we calculated CI according to the Chou-Talalay method[29] using CalcuSyn software (Biosoft, Cambridge, UK). CI allows for quantitative definition of drug interactions; antagonism (CI>1), additive effect (CI = 1) and synergism (CI<1).

3.5.3. Apoptotic assay

Apoptotic rates were assessed by flow cytometry using the annexin V–fluorescein isothiocyanate (annexin V - FITC)/propidium iodide (PI) kit (BD Pharmingen), in which annexin V binds to exposed phosphatidylserines of early apoptotic cells, whereas PI stains cells that have increased membrane permeability, i.e., late apoptotic or necrotic cells. Samples were prepared according to the manufacturer's instructions. Flow cytometry analysis was performed using a FACS-Calibur cytometer (Becton Dickinson). The annexin V+/PI- cells were defined as early apoptotic cells.

3.5.4. Flow-cytometric analysis of cell phase distribution

Quantitative analysis of cell cycle phase distribution was performed by flow-cytometric analysis of the DNA content in fixed of K562 cells, after staining with PI (Sigma-Aldrich).[47] Cells in an exponential growth phase, at a density of 2 x 10^5 cells/Petri dish (dimensions 60 x 15 mm, NUNC) were continually exposed to investigated hit compounds at concentrations of 70 µM. After indicated times of continual treatment, cells were collected by trypsinization, washed twice with ice-cold PBS, and fixed for 30 min in 70% EtOH. Fixed cells were washed again with PBS, and incubated with RNase A (1 mg/mL) for 30 min at 37°C. Just before flow-cytometric analysis, the cells were stained with PI at a concentration of 400 µg/mL. Cell cycle phase distributions were analyzed using a FACS Calibur Becton Dickinson flow cytometer and Cell Quest computer software.

3.5.5. Clonogenic Assay for Proliferation Ability

After 24 h treatment of K562 cells with compound **5** the cells were washed with PBS, and resuspended in Cell Resuspension Solution (R&D Systems). Briefly, 0.5 × 10^4/mL treated K562 cells were mixed with 1 mL of Human methylcellulose complete medium (R&D Systems). Cells were then plated in a 35 mm plastic dish (Falcon). The blast colonies (> 50 cells) of K562 cells were scored on day 7. All assays were performed in duplicate.

Acknowledgments

This project was supported by the Ministry of Education, Science and Technological Development of the Republic of Serbia, Contract #173001 and # 172033. This work was also partially supported by the University of Parma (to MR) and by Turku University Hospital (to MS). ST is supported by a fellowship from the Chiesi Foundation. The COST Actions CM1207 is also kindly acknowledged for supporting the short term scientific mission of JV to MR laboratories. Dr. Emmanuele Crespan and Dr. Jorge I. Armijos Rivera are kindly acknowledged for the enzymatic screening on two unrelated targets: the oncogenic Src and Abl kinases.

References and notes

1. Ernsberger, P.; Giuliano, R.; Willette, R. N.; Reis, D. J. *J. Pharmacol. Exp. Ther.* **1990**, 253, 408.
2. Bousquet, P.; Bricca, G.; Dontenwill, M.; Feldman, J.; Belcourt, A.; Tibiriça, E. *Therapie* **1992**, 47, 525.
3. Head, G. A.; Mayorov, D. N. *Cardiovasc. Hematol. Agents Med. Chem.* **2006**, 4, 17.
4. Chan, C. K.; Burke, S. L.; Head, G. A. *J. Hypertens.* **2007**, 25, 147.
5. Aceros, H.; Farah, G.; Noiseux, N.; Mukaddam-Daher, S. *Eur. J. Pharmacol.* **2014**, 740, 168.
6. Zaitseva, I. I.; Størling, J.; Mandrup-Poulsen, T.; Berggren, P. O.; Zaitsev, S. V. *Cell. Mol. Life Sci.* **2008**, 65, 1248.
7. McLean, L. S.; Crane, L.; Baziard-Mouysset, G., Edwards, L. P. *Pharmacol. Rep.* **2014**, 66, 937.
8. Srdic-Rajic, T.; Nikolic, K.; Cavic, M.; Djokic, I.; Gemovic, B.; Perovic, V.; Veljkovic, N. *Eur. J. Pharm. Sci.* **2016**, 81, 172.
9. Piletz, J. E.; Jones, J. C.; Zhu, H.; Bishara, O.; Ernsberger, P. *Ann. N.Y. Acad. Sci.* **1999**, 881, 1.
10. Alahari, S. K. *Exp. Cell. Res.* **2003**, 288, 415.
11. Baranwal, S.; Wang, Y.; Rathinam, R.; Lee, J.; Jin, L.; McGoey, R.; Pylayeva, Y.; Giancotti, F.; Blobe, G. C.; Alahari, S. K. *J. Natl. Cancer Inst.* **2011**, 103, 1513.
12. Hortobágyi, G. N. *Drugs* **1997**, 54, 1.
13. Weiss, R. B. *Semin. Oncol.* **1992**, 19, 670.
14. Gianni, L.; Dombernowsky, P.; Sledge, G.; Martin, M.; Amadori, D.; Arbuck, S. G.; Ravdin, P.; Brown, M.; Messina, M.; Tuck, D.; Weil, C.; Winograd, B. *Ann. Oncol.* **2001**, 12, 1067.
15. Seidman, A.; Hudis, C.; Pierri, M. K.; Shak, S.; Paton, V.; Ashby, M.; Murphy, M.; Stewart, S. J.; Keefe, D. *J. Clin. Oncol.* **2002**, 20, 1215.
16. Nikolic, K.; Veljkovic, N.; Gemovic, B.; Srdic-Rajic, T.; Agbaba, D. *Comb. Chem. High Throughput Screen.* **2013**, 16, 298.
17. Veljkovic, V.; Veljkovic, N.; Esté, J. A.; Hüther, A.; Dietrich, U. *Curr. Med. Chem.* **2007**,14, 441.
18. Veljkovic, V.; Mouscadet, J. F.; Veljkovic, N.; Glisic, S.; Debyser, Z. *Bioorg. Med. Chem. Lett.* **2007**, 17, 1226.
19. Veljkovic, V.; Loiseau, P. M.; Figadere, B.; Glisic, S.; Veljkovic, N.; Perovic, V. R.; Cavanaugh, D. P.; Branch, D. R. *F1000Res.* **2015**, 2, 4.
20. Cross, S.; Baroni, M.; Carosati, E.; Benedetti, P.; Clementi, S. *J. Chem. Inf. Model* **2010**, 50, 1442.
21. Sirci, F.; Goracci, L.; Rodríguez, D.; van Muijlwijk-Koezen, J.; Gutiérrez-de-Terán, H.; Mannhold, R. *J. Comput. Aided Molec. Des.* **2012**, 26, 1247.
22. Sirci, F.; Istyastono, E. P.; Vischer, H. F.; Kooistra, A. J.; Nijmeijer, S.; Kuijer, M.; Wijtmans, M.; Mannhold, R.; Leurs, R.; de Esch, I. J.; de Graaf, C. *J. Chem. Inf. Model.* **2012**, 52, 3308.
23. Sciabola, S.; Stanton, R. V.; Mills, J. E.; Flocco, M. M.; Baroni, M.; Cruciani, M. G.; Perruccio, F.; Mason, J. S. *J. Chem. Inf. Model.* **2010**, 50, 155.
24. Drwal, M. N.; Griffith, R. *Drug Discov. Today Technol.* **2013**, 10, e395.
25. Pieroni, M.; Machado, D.; Azzali, E.; Santos Costa, S.; Couto, I.; Costantino, G.; Viveiros, M. *J. Med. Chem.* **2015**, *58*, 5842.
26. Molderings, G. J.; Göthert, M.; von Kügelgen, I. *Pharmacol. Rep.* **2007**, 59, 789.
27. Irwin, J.J.; Duan, D.; Torosyan, H.; Doak, A.K.; Ziebart, K.T.; Sterling, T.; Tumanian, G.; Shoichet, B.K. *J.Med.Chem.* **2015**, *58*, 7076.
28. De Oliveira, F.; Chauvin, C.; Ronot, H.; Mousseau, M.; Leverve, X., Fontaine, E. *Oncogene* **2006**, 25, 2646.
29. Chou, T.C. *Cancer Res.* **2010**, 70, 440.
30. Songsiang, U.; Thongthoom, T.; Boonyarat, C.; Yenjai, C. *J. Nat. Prod.* **2011**, *74*, 208.
31. Nagarapu, L.; Gaikwad, H.K.; Sarikonda, K.; Mateti, J.; Bantu, R.; Raghu, P.S.; Manda, K.M.; Kalvendi, S.V. *Eur. J. Med. Chem.* **2010**, *45*, 4720.
32. Caruso, A.; Sinicropi, M.S.; Lancelot, J.C.; El-Kashef, H.; Saturnino, C.; Aubert, G.; Ballandonne, C.; Lesnard, A.; Cresteil, T.; Dallemagne, P.; Rault, S. *Bioorg. Med. Chem. Lett.* **2014**, *24*, 467.
33. Yoon, S.; Kim, J.H.; Lee, Y.J.; Ahn, M.Y.; Choi, G.; Kim, W.K.; Yang, Z.; Lee, H.J.; Moon, H.R.; Kim, H.S. *Eur. J. Pharmacol.* **2012**, 697, 24.
34. Radi, M.; Vallerini, G. P.; Petrelli, A.; Vincetti, P.; Costantino, G. *Tetrahedron Lett.* **2013**, 54, 6905.
35. Schüller, A., Schneider, G.; Byvatov, E. *QSAR Comb. Sci.* **2003**, 22, 719.
36. http://www.vin.bg.ac.rs/180/tools/formcalc.php (accessed 15.03.2015).
37. Baroni, M.; Cruciani, G.; Scabiola, S.; Perruccio, F.; Mason, J. S. *J. Chem. Inf. Model* **2007**, 47, 279.
38. http://www.moldiscovery.com/product/manual/flap/ (accessed 10. 12. 2015).
39. Jain, A. N.; Nicholls, A. *J. Comput. Aided Molec. Des.* **2008**, 22, 133.
40. Pohjanoksa, K.; Jansson, C. C.; Luomala, K.; Marjamäki, A.; Savola, J. M.; Scheinin, M. *Eur. J. Pharmacol.* **1997**, 335, 53.
41. Bradford, M. M. *Anal. Biochem.* **1976**, 72, 248.
42. Peltonen, J. M.; Pihlavisto, M.; Scheinin, M. *Eur. J. Pharmacol.* **1998**, 355, 275.
43. Cheng, Y.; Prusoff, W. H. *Biochem. Pharmacol.* **1973**, 22, 3099.
44. Mosmann, T. *J. Immunol. Methods* **1983**, 65, 55.
45. Ohno, M.; Abe, T. *J. Immunol. Methods* **1991**, 145, 199.
46. Eshkourfu, R.; Čobeljić, B.; Vujčić, M.; Turel, I.; Pevec, A.; Sepčić, K.; Zec, M.; Radulović, S.; Srdić-Radić, T.; Mitić, D.; Andjelković, K.; Sladić, D. *J. Inorg. Biochem.* **2011**, 105, 1196
47. Ormerod, M. G. Oxford University Press, New York, **1994**; pp 119 125.

Supplementary Material

Supplemental information entails: (1) I_1-IR ligands used in VS study and corresponding binding affinities ($pK_i = \log(1/K_i)$), (2) ^{1}H-NMR spectra, (3) Evaluation of proapoptotic activities of moxonidine and efaroxan and (4) Enzymatic assays on isolated Src and Abl kinases.

HIGHLIGHTS

- **Identification of rilmenidine-derived compounds with antitumor activity**
- **Combined VS singled out 11 candidates that were synthesized and in vitro tested**
- **Examined compounds haven't shown any significant activity on α_{2A}-adrenoceptors**
- **The most active compound 5 exhibited a cytotoxic profile similar to rilmenidine**
- **Compound 5 combined with doxorubicin demonstrated synergism in evoking apoptosis**